Terahertz Irradiation of Liquid Water Inhibits Methane Hydrate Formation

Pietro Di Profio,* Valentino Canale, Michele Ciulla, Antonella Fontana, Luca Madia, Massimo Zampato, and Stefano Carminati*

Cite This: https://doi.org/10.1021/acssuschemeng.2c00994

Read Online

ACCESS | Metrics & More | Article Recommendations

ABSTRACT: In the general effort toward a low carbon economy, natural gas (NG) may represent a viable solution in a transition scenario. NG is conveyed through pipelines where, under low temperatures and high pressures that are typically found under sea bottom conditions (1−4 °C and 6−8 MPa), ice-like solid gas hydrates may form, grow, accumulate, and eventually cause complete pipe plugging. To avoid such events, chemical inhibitors are generally added, which chemically disrupt the structure of water, preventing the formation and/or growth of hydrates. To identify alternative chemical-free approaches to hydrate inhibition, the effects of electromagnetic radiation in the terahertz (THz) domain are explored. In this paper, we show, for the first time, that hydrate formation is inhibited by irradiating the water/methane system with THz radiation in the spectral region between 1 and 5 THz. In addition, we show that this inhibition persists for many hours after switching off the irradiation. A tentative explanation of this phenomenon is given in terms of THz radiation interaction with vibrational modes of water in hydrate-like cages. The findings reported herein may be developed into a sustainable, chemical-free hydrate inhibition process.

KEYWORDS: hydrate inhibition, terahertz radiation, chemical-free process, gas production, pipeline plugging
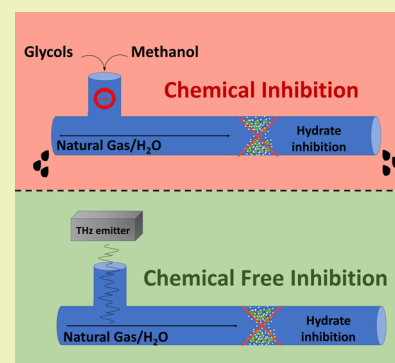
INTRODUCTION

Global decarbonization initiatives are on the agendas of worldwide governments. Most aggressive projections set a reduction of 75% in hydrocarbon production by 2050 with respect to current levels.[1] In this scenario, natural gas will probably maintain 50% of actual production mainly for power generation, industrial use, and hydrogen production. A major issue in its transportation through pipelines is the formation of clathrate hydrates that naturally form under subsea conditions (pressure values of 6−8 MPa and temperatures around 1−4 °C). Without an injection of chemical inhibitors, hydrates may accumulate and eventually cause complete pipeline plugging. Clathrate hydrates are supramolecular compounds formed when small (usually gaseous) molecules, such as methane, carbon dioxide, and hydrogen, interact with water under defined pressure and temperature conditions. Solutions adopted to manage hydrate-related problems are based on lowering the hydrate formation temperature with the use of chemicals (thermodynamic inhibitors, TIs) or interfering with hydrate growth by employing polymers or small molecules (low-dosage hydrate inhibitors, LDHIs). TIs are basically methanol or glycols, which reduce hydrate formation by establishing hydrogen bonds with water molecules. TIs are added in huge amounts into the production wells and portions of pipelines, and for this reason, they represent both an economic burden and an environmental risk in case of

accidental spills.[2,3] LDHIs have been developed in an attempt to overcome some issues posed by TIs.[4−8] They are generally small- to medium-sized surfactants or polymers, which act specifically by interfering with the agglomeration of hydrate crystallites, thus delaying the formation of bulk hydrates.[9,10]

Sloan[11,12] proposed that hydrate formation starts as an interplay among cage-like water clusters, which are normally present in liquid water, and guest molecules (e.g., methane) leading to a reorganization process to form clathrate crystallites. Molinero et al.[13,14] modeled hydrate formation and pointed out that this process, at its very first stage, is characterized by pairs of methane molecules stabilized by pentagonal and hexagonal water rings leading to larger aggregates, called "blobs", that eventually grow into massive hydrate. Methane (or other guests) molecules are then critical for hydrate formation.

These models suggest that the presence of structured water, in the form of rings or clusters, is a prerequisite for hydrate formation. Experimental evidence indicates that this process
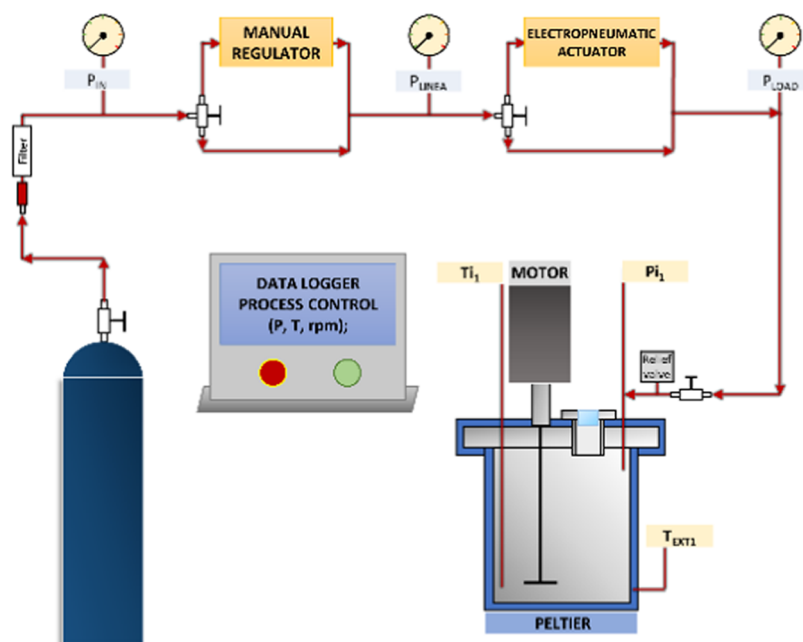
Figure 1. Experimental setup.

starts at the gas/water interface, where ordered water structures have been identified by neutron and laser reflectivity experiments.[15] The work of Hassanali[16] gives computational evidence of the presence of stable voids in liquid water able to accommodate hydrophobic molecules, where water molecules may organize in spherical or branched cavities. Recent papers point to the coupling of THz radiation with low-energy collective modes of water[17] and its clusters,[18] as well as the use of THz spectroscopy for the study of interactions between water molecules and simple hydrocarbons as a model of clathrate hydrate host–guest interactions.[19]

Interaction energies between hydrate cage-forming water molecules and guest species, such as methane and carbon dioxide, have been recently studied using the density functional theory (DFT) approach.[20] In particular, the authors show that vibrational frequencies of the Raman spectra of water in the region 2600–3000 cm^{-1} shift according to the kind of guest and the type of cage formed. Importantly, they show that THz radiation could destabilize the hydrogen-bonding network of the cages, thus leading to the release of methane molecules from clathrates. Indeed, it has been reported by Johnson[21,22] that THz irradiation could lead to the weakening of clathrate hydrogen bonds by closing the energy gap between the highest occupied molecular orbitals (HOMOs) and the lowest unoccupied molecular orbitals (LUMOs) of water clusters that resemble the dodecahedral hydrate structures (see below), thus resulting in a disruption of hydrate cages.

Recently, Zhang and co-workers[23,24] have also carried out a DFT study, observing that two kinds of vibrational modes of H-bonded water exist in sI methane hydrates and ice XVII, which is similar to sI hydrates but with no guest molecules. These are a stronger, four-bond mode at 291 cm^{-1} and a weaker, two-bond mode at 210 cm^{-1} (8.72 and 6.30 THz, respectively). They also noticed that liquid water does not show such H-bond vibration modes in this region due to the lack of a rigid tetrahedral structure, concluding that THz irradiation could specifically target hydrate cage H-bonds, leaving bulk water unaffected. The negligible "thermal" effect

upon THz irradiation of water allows us to exclude the increase of temperature as the cause of hydrate cage disruption.[25] Johnson[22] also specifically refers to water pentagonal dodecahedral $(H_2O)_{21}H^+$ clusters in water vapor that, when optically excited, emit strong THz radiation. These clusters, which have been observed also in the liquid phase, are formally identical to the 5^{12} cage of clathrate hydrates.[12]

Water is also known for manifesting an abnormally high dielectric permittivity.[26,27] The characteristic dielectric loss in the range of 20–200 GHz has been recently simulated as the result of two main physical processes, namely, the motion of single water molecules and collective dynamics of hydrogen-bonded water clusters.[27] Lunkenheimer et al.[26] approached the controversial subject of mm to sub-mm radiation absorption by water by conducting dielectric, terahertz, and far-IR spectroscopies at temperatures from 275 to 350 K and at ambient pressure and observed complex spectra which could be deconvoluted at lower temperatures to obtain information on the contributing physical processes. The main relaxation at 20–100 GHz should be a nearly Debye-type process by which molecular (water) units reorient their dipoles. They also observed several other absorptions above 1 THz, which are related to collective motions of water clusters (see Discussion).

Based on the evidence that THz may strongly interact with water hydrogen bonds and considering that hydrates form through an aggregation process,[13,14] in this paper, we show, for the first time, that THz irradiation can inhibit methane hydrate formation without using any chemicals under experimental conditions of moderate driving force, i.e., less than 2.1 MPa above the equilibrium pressure. Inside the hydrate formation zone, with a continuous exposure for 48 h of water and methane to THz radiation in the 1–5 THz range, methane hydrate formation was totally inhibited, with this inhibition persisting for several days after switching off the radiation source. Remarkably, hydrate inhibition was also observed when water was irradiated for limited times (120 min or less) inside and outside the hydrate formation zone and before submitting to pressure/temperature hydrate-forming conditions. After

proper development and optimization, a THz-based inhibition process could lead to completely sustainable, chemical-free flow assurance operations in the field of oil and gas production.

EXPERIMENTAL SECTION

Materials. CH_4 (2.5 grade, >99.5% methane) was purchased from SOL S.p.A. (SOL Spa, Monza (MB), Italy). Ultrapure water was imported from a Direct-Q device (Millipore, Burlington, MA, U.S.A.).

Reactor. Hydrate formation was carried out in a fully controlled, AISI 316L stainless steel reactor designed and assembled by RDPower SRL (Terni, Italy) (Figure 1), with an internal volume of 0.5 L and an operating pressure of up to 20 MPa. The cooling/heating system was a Peltier unit, which allowed the operating temperature ranging from 253 to 353 K.

A chiller with a cooling power of 1000 W was used as a heat sink for the Peltier units. The internal stirring was carried out with a magnetic-coupled stir bar (50−800 rpm). Gas flow was controlled by a CC series micrometering valve (Tescom). Gas replenishment during hydrate formation was done by a combination of a Kammer electropneumatic actuator and a low-flow globe valve, both from Flowserve. Before and after the metering valve, two pressure transducers were mounted to check the pressure along the gas line. Reported pressures are absolute values. A resistive temperature detector (RTD) PT100 class 1/3 DIN (OMEGA Engineering, INC.) was also installed. An in-house process controller for pressure, temperature, and gas flow was assembled using an ELCO Top 7 PLC (ELCO, Italy). The controller allowed to set the temperatures of the reactor and drive the Peltier power supply to apply cooling or heating power as required. The temperature set point was maintained using a PID algorithm embedded into the PLC controller, joined to an algorithm conceived to minimize thermal oscillations during hydrate formation.

Femtosecond Laser. THz waves were generated by optical rectification, a nonlinear process that consists in the generation of a quasicontinuous polarization in a nonlinear medium at the passage of an intense optical beam. When the applied electric field is delivered by a femtosecond pulsed laser, the spectral bandwidth associated with such short pulses is very large. The mixing of different frequency components produces a beating polarization, which results in the emission of electromagnetic waves in the THz region (Figure 2).
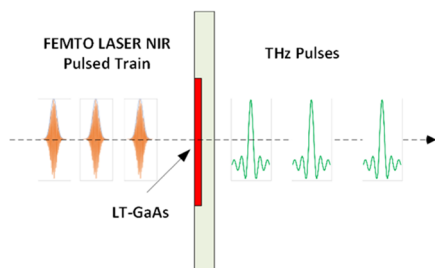

Figure 2. THz generation from femtosecond laser pulses.

The laser source is a femtosecond FiberPro NIR (Toptica Photonics Ag, Germany) based on a SAM mode-locked ring oscillator. Laser pulses are carefully amplified to very high peak powers in a subsequent core-pumped fiber amplifier. This laser provides elevated peak power levels at pulse widths well below 100 fs, and it includes an additional exit aperture with a single-pass second harmonic generation (SHG). The unit delivers a collimated free beam with more than 350 mW at 1560 nm fundamental wavelength ($P_{Out}^{1560\,nm} > 350$ mW) and the second harmonic of 780 nm ($P_{Out}^{780\,nm} > 140$ mW). The laser has been installed above the quartz window of the reactor as shown in Figure 3.

THz Antenna. The antenna used for the generation of THz waves consists of a microstrip photoconductive antenna realized on a low-temperature-grown GaAs (LT-GaAs) substrate (TeraVil Ltd., Lithuania), with the following specifications:
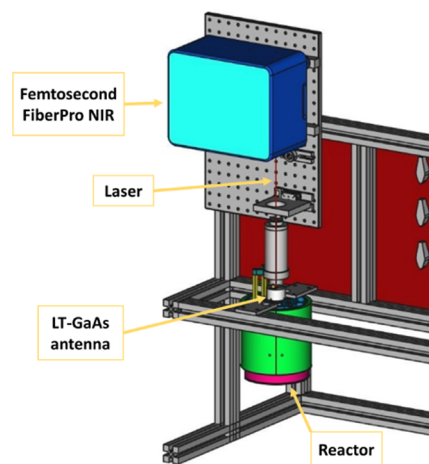

Figure 3. Laser configuration and assembly onto the reactor.

- Wafer dimensions: 5 ×1.5 mm typical
- Power: 10 μW typical @30 mW pump and 40 V bias
- Pumping wavelength: 800 ± 40 nm

The THz emitter was operated by focusing thereon the previously described laser by adjusting its power suitably to avoid crystal damage. The THz antenna (Figure 4) was mounted a few millimeters above
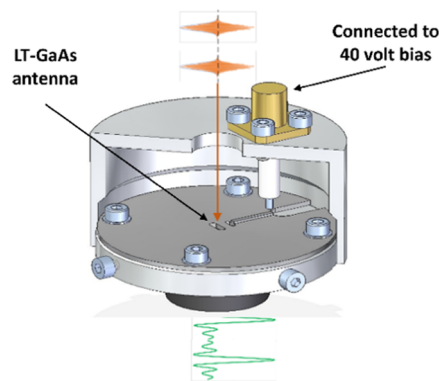

Figure 4. Setup for THz emitter.

the window of the reactor. THz radiation was collected by an integrated divergent lens, manufactured from high-resistivity silicon (HRFZ-Si) to cover the irradiated water surface.

THz radiation intensity was modulated through the pumping power regulator. Tests were performed at 7.5 and 11 mW pump with 30 V bias. No direct THz intensity measurements are available. With this laser excitation, THz powers expected are in the range around 0.1 and 1.0 μW.[28] A silicon carbide hemisphere set directly below the antenna blocks any laser transmission to the sample.

Experimental Method. Methane hydrates form under specific pressure and temperature conditions. For a given gas composition, driving forces are related to pressure and temperature: hydrates form by increasing pressure (overpressurizing) and/or decreasing temperature (subcooling) with respect to the formation equilibrium curve (Figure 5). In Figure 5, the pressure and temperature conditions adopted in our experiments are reported as the point H.

The driving force to hydrate formation was set overpressurizing the system at a constant temperature. Figure 6 shows a typical evolution of pressure and temperature for a water/methane system entering the hydrate formation zone. Starting from a nonhydrate-forming condition, e.g., 5.6 MPa and 10 °C, after an equilibration time, the temperature is decreased to enter the pressure/temperature formation zone, where P drops slightly due to cooling. This P/T set point is maintained until the hydrate starts forming. This procedure is
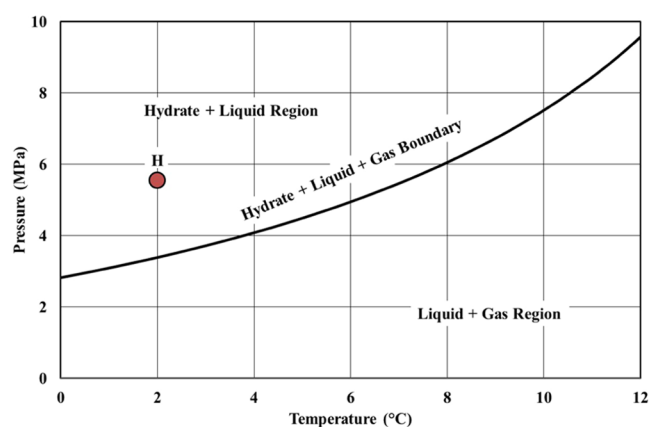
Figure 5. Pressure/temperature diagram for hydrate-forming conditions. Point H: P/T gas hydrate conditions in this work. Overpressure with respect to the boundary curve of 2.1 MPa. The theoretical curve was generated with CSMHYD software.[29]
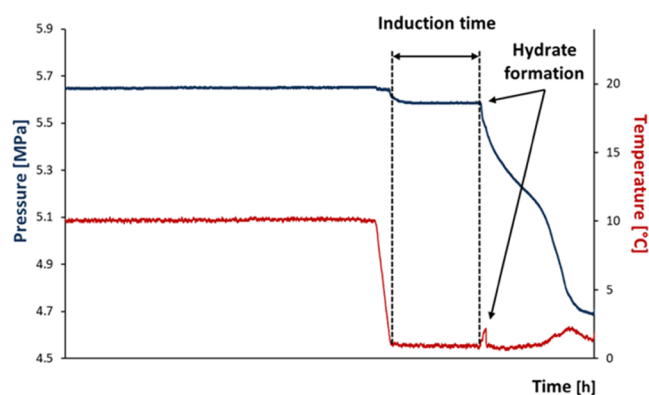

Figure 6. Typical gas hydrate formation experiment. After equilibration at 5.6 MPa and 10 °C, the water/methane system is cooled to 2 °C. Pressure slightly decreases due to the temperature decrease (closed vessel), and the system reaches the gas hydrate formation zone (GHFZ). Hydrates start forming after some time called the induction time.

commonly used both in academia and industry to measure hydrate formation times and test chemicals that delay/inhibit their massive formation and is referred to as the induction time measure-ment,[11,30,31] which consists in the measurement of the time elapsed until hydrate formation after the system reaches the P/T set point. Induction time reflects the latency before the hydrate begins to grow massively and rapidly, corresponding to a marked pressure drop and a visible exothermic peak (Figure 6): induction time starts at the temperature set point, first dashed bar at 2 °C, and ends at the second dashed bar, corresponding to the beginning of the exothermic peak.

Figure 7 shows the complete P/T cycle used in this work to bring the water/methane system in the hydrate formation region. The water-filled (100 mL) reactor was kept at 20 °C and connected to line vacuum for 2 h while stirring and then fluxed with methane at 20 °C. It was then pressurized with methane at a pressure ramping rate of 0.1 MPa/min up to 5.6 MPa. After reaching the pressure set point (5.6 MPa), the system was cooled to 10.0 °C at a cooling rate of 1 °C/min, with methane pressure maintained constant through an electropneumatic device. Temperature and pressure were then kept constant for 2 h. Finally, the system was cooled to 2 °C (cooling rate of 0.4 °C/min), and, after closing the electropneumatic valve, the internal pressure slightly decreased to 5.4 MPa. By closing the electropneumatic valve, the system is shifted from constant pressure to pressure dropping conditions in the gas hydrate formation zone (GHFZ), where pressure reduction reflects methane hydrate formation.

We chose three possible irradiation periods with THz radiation: continuous irradiation, starting as soon as the system reaches the set point until the end of the experiment; period A, which is irradiation for a set time before entering the GHFZ; and period B, consisting of irradiation for a set time within the GHFZ (Figure 7). THz radiation was applied onto the water surface in the reactor at different irradiation durations and radiation powers (see details in the Results section).

■ RESULTS

Hydrate Formation Cycle (No THz Irradiation). It is well known from the literature that the first nucleation events in hydrate formation are stochastic phenomena that can be hardly modeled and predicted.[11] To establish a common reference and overcome the inherent variability that could make the comparison of results questionable, in each experiment, we used freshly prepared deionized, distilled water. This, together with water degassing, finely controlled temperature, pressure, and stirring parameters (see Experimental Section), gives us an acceptable range of variability in defining our reference in the hydrate induction time. Figure 8 reports the means and standard deviation of the induction time (see Figure 6) measured in nine experiments, showing a
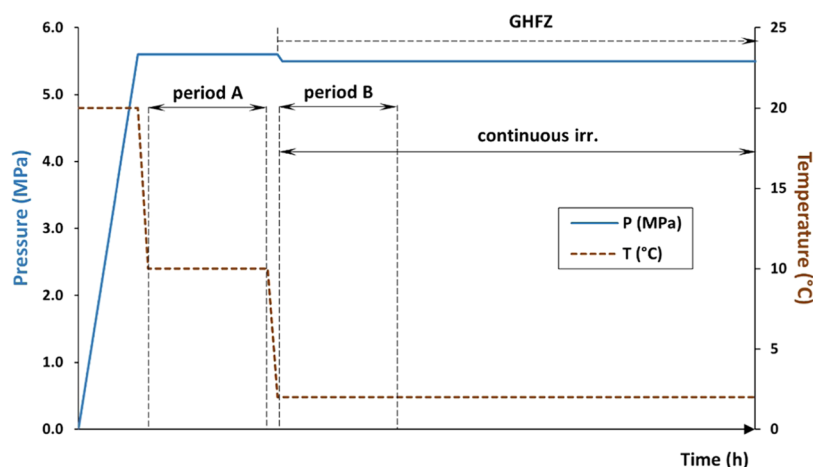

Figure 7. Complete P/T cycle for the hydrate formation experiment. "Continuous irr." means continuous irradiation throughout the experiment; periods A and B refer to irradiation periods outside and inside the GHFZ, respectively. Overpressure is reported in Figure 5.
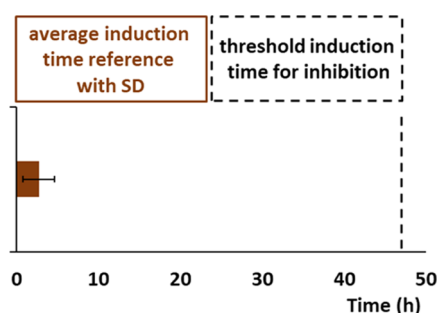
Figure 8. Average induction time for nine experiments (2.76 ± 2.59 h) for noninhibited water (brown) compared with the induction time threshold to be reached for considering the experiment as inhibited.

relatively narrow dispersion of values with respect to data reported in the literature.[11] Hydrate formation was considered inhibited when the induction time reached a threshold value of 48 h, well above our reference, noninhibited hydrate induction times.

Inhibition Effect: Continuous THz Irradiation within the Gas Hydrate Formation Zone. The P/T diagram of Figure 9 shows the effect of THz irradiation in the GHFZ. For each test, fresh water and methane were used and a reference hydrate formation was carried out before each replicate. For the sake of clarity, only one exemplary curve (red) is reported in the figure. Methane pressure decreases when the clathrate hydrate is formed (Figure 9, red curve). Yellow, orange, and blue curves refer to the effect of continuous THz irradiation, where no pressure variation is recorded, thus reflecting complete hydrate inhibition (no appreciable clathrate formation).

The reference experiment (red line) shows that the formation starts after an induction time of ca. 3 h, where the pressure inside the reactor drops from ca. 5.50 to 3.10 MPa due to the significant methane hydrate formation. After running the reference experiment, the system was returned

to ambient temperature, and the P/T cycle was repeated turning on the femtosecond laser-induced THz emitter (11 mW, 30 V bias) when P/T gas hydrate-forming conditions were reached. In contrast to what happened in the reference experiment (without irradiation), no hydrate formation was observed under THz irradiation for 48 h in two consecutive cycles (yellow and orange curves) until the end of the experiment. In the third cycle, the sample was left under irradiation for 90 h, observing persistence of inhibition also after this longer time (blue curve).

Hydrate Inhibition Persistency with Shorter Irradiation Times (Periods A and B). To investigate whether the hydrate inhibition could persist even after switching off THz irradiation, the water/methane system was driven to the GHFZ P/T set point and irradiated for 2 h (see irradiation period B in Figure 7), and then hydrate formation was monitored. As shown in Figure 10, 2 h of irradiation in the GHFZ completely inhibited hydrate formation for at least 48 h (the allotted time for each experiment). Table 1 shows the results of repeated experiments.

To better explore THz effects under different conditions, the water/methane system was irradiated before entering the GHFZ (period A at 10 °C, 5.6 MPa) with two different values of laser power (11 and 7.5 mW) and two irradiation times (2 h and 20 min). Complete inhibition under hydrate-forming conditions after 2 h of irradiation in period A was obtained for more than 48 h even at a lower laser power (7.5 mW) (Table 2). Decreasing irradiation time in period A down to 20 min, inhibition could not be always achieved (Table 3), thus possibly indicating that this irradiation time/laser power (7.5 mW/20 min) may be considered as a threshold at which THz irradiation starts to be less effective in inhibiting hydrate formation.

■ DISCUSSION

In this work, we present an experimental evidence that hydrate formation can be inhibited by irradiating the liquid water/
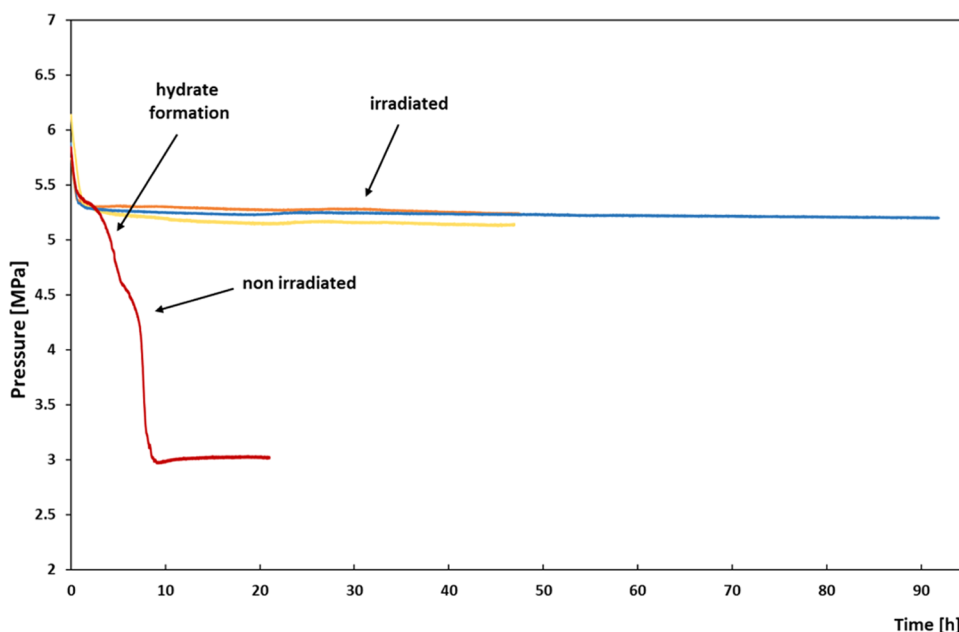

Figure 9. (a) Red curve represents hydrate formation without irradiation and (b) yellow, orange, and blue curves are under THz irradiation in the GHFZ P/T set point.
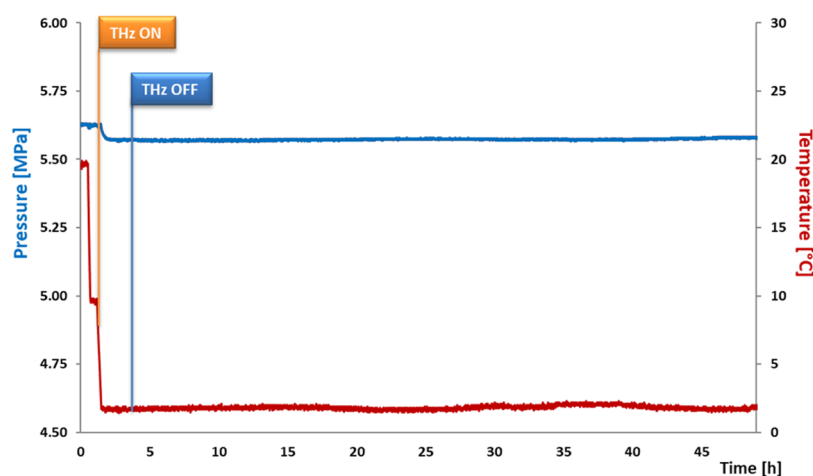
Figure 10. Hydrate inhibition persisted for at least 48 h after 2 h of THz irradiation (period B).

Table 1. Repeated Hydrate Inhibition Persistency Tests: Irradiation Started at the P/T Set Point of the GHFZ and Lasted for 2 h (Irradiation Period B)[a]

exp. no	irradiation period	irradiation duration (h)	THz source (laser power mW)	Inhibition persistency after switching off the THz source (h)
1 to 4	B	2	11	≥48

[a]Inhibition persisted at least for 48 h after switching off the THz source.

methane system with electromagnetic radiation in the low THz range. Surprisingly, we also found that such inhibition persisted for at least 48 h after switching off the irradiation. This frequency range has been already suggested to dissociate clathrate hydrates, as claimed by Johnson,[21] while Aparicio et al.[20] proposed that the energy gap between the HOMO and LUMO of a hydrate (or hydrate-like) cage is closed by the vibrations induced by irradiation in the range around 1−10 THz, thus allowing transfer of electrons from the bonding into the antibonding orbitals and causing the release of methane from clathrate cages. We might expect that this disruption should be effective only in the presence of hydrate, but our experiments show that it is possible to interfere with this process by acting just before hydrate formation, specifically when water is structuring around methane molecules (i.e., Molinero's blobs), where pentagonal and hexagonal water rings, and possibly larger structures, seem to play a key role during hydrate nucleation. An effect of heating due to THz irradiation could be excluded according to Zhang et al.,[23,24] who show a lack of absorption peaks in the range 200−300 cm^{-1} (about 6−9 THz) for liquid water, thus suggesting that irradiation with 1−10 THz should not increase the temperature of the system, as confirmed by other authors.[25] The present results are a confirmation that THz waves inhibit the evolution of H-bonded water clusters toward macroscopic

hydrates and may find an explanation in the fact that those pentagonal/hexagonal structures bear resemblance to 5^{12} cages or $(H_2O)_{20}$ clusters that have been shown to interact with THz radiation. More surprising is the fact that such an inhibition is persistent for several (i.e., at least 48) hours after stopping the irradiation. This relatively long-lived phenomenon is not a trivial finding, and we do not have a straightforward explanation. The work by Lunkenheimer et al.[26] shows that absorption of frequencies centered around 1.8 THz may be caused by phonon excitations of water clusters (e.g., $(H_2O)_{20}H^+$) into resonant phonon (i.e., vibrational) modes of the same frequency.[22] Above 3 THz, the absorption can be ascribed to hydrogen-bond stretching (5 THz) and librational motions (20 THz). Yu et al.[32] showed a clear absorption mode of water around 1.56 THz. This mode should be related to the bending motion of the hydrogen bonds that keep water cages together. Irradiation of clathrate hydrates with 6−10 THz radiation was also reported to decompose the hydrate through resonant absorption due to vibrational modes similar to those observed at 6.8 and 9.1 THz in ice Ih, XVI, and XVII.[23]

Photoacoustic wave generation in water has been recently reported following irradiation of the water surface with loosely focused, low-energy terahertz radiation (3−7 THz, <1 mJ/cm^2).[33] This phenomenon has been ascribed to linear absorption of THz light by water in the first 10 μm of water surface, which is due to the resonance of intermolecular vibrations of hydrogen-bonded water cages. This absorption generates a rapid pressure increase, giving rise to a photoacoustic wave that propagates for several millimeters below the surface, and has been proposed as a means for affecting chemical processes (e.g., hydrate formation) within the bulk water. The reported photoacoustic phenomenon may also be related to the resonant phonon modes of THz-excited water clusters, as discussed above.[26] Perturbation of hydrate formation by acoustic processes (photoacoustic waves, phonons) may explain the effectiveness of hydrate inhibition also in the bulk water and not only at its surface because they

Table 2. Gas Hydrate Inhibition after THz Irradiation in Period A[a]

exp. no	irradiation period	irradiation duration (h)	THz source (laser power mW)	inhibition persistency recorded in the GHFZ (h)
5−7	A	2	11.0	≥48
8−10	A	2	7.5	≥48

[a]Inhibition persisted for more than 48 h when the water/methane system was in the GHFZ.

Table 3. Gas Hydrate Inhibition Test after THz Irradiation in Irradiation Period A at Reduced Laser Power and Shorter Irradiation Time

exp. no	irradiation period	irradiation duration (min)	THz source (laser power mW)	inhibition persistency recorded in the GHFZ (h)
11	A	20	7.5	≥48
12	A	20	7.5	40
13	A	20	7.5	2

propagate into the water body much deeper than the incident THz radiation.

Some theoretical works[34−36] point out the possibility that the interaction of electromagnetic fields with matter (water) may set up a coherent state composed of relatively macroscopic, long-lived phases arranged in a periodic lattice. Such phases or domains could therefore hamper the reorganization of water into crystal-like aggregates such as hydrate clusters. However, this approach to water structuring is deeply controversial in the literature.[37]

■ CONCLUSIONS

Our experiments show that under mild driving force conditions, water continuously exposed to THz irradiation is not able to reorganize itself into structures conducive to hydrates, possibly by disrupting 5^{12}-like water clusters through the induction of specific vibrational modes of the cluster's H-bonds and/or by closing the HOMO−LUMO energy gap of water clusters and smaller structures. It may be argued that a fraction of liquid water may exist as ordered structures that "seed" hydrate formation. Once disrupted by THz irradiation, this fraction loses the ability to form hydrates. Incidentally, the availability of these structures may naturally change in unperturbed liquid water, this being a possible factor determining the well-known stochastic nature of induction times in hydrate formation, as reported in the literature.[12]

These findings need further confirmation by a different, high-throughput approach, allowing us to gather more experimental information, combined with structural investigation. We suggest that electromagnetic irradiation in the THz domain may have the potential for developing a sustainable chemical-free, low-cost technology for hydrate prevention in flow assurance. Other research fields could also take advantage of these results, particularly in biology, where THz-modified water may have a significant impact on aggregation phenomena and/or biochemical reactions.

■ AUTHOR INFORMATION

Corresponding Authors

Pietro Di Profio − *Department of Pharmacy, University of Chieti-Pescara "G. d'Annunzio", I-66010 Chieti, Italy;* orcid.org/0000-0002-8038-7940; Email: pietro.diprofio@unich.it

Stefano Carminati − *Eni S.p.A., I-20097 Milan, Italy;* Email: stefano.carminati@eni.com

Authors

Valentino Canale − *Department of Pharmacy, University of Chieti-Pescara "G. d'Annunzio", I-66010 Chieti, Italy*

Michele Ciulla − *Department of Pharmacy, University of Chieti-Pescara "G. d'Annunzio", I-66010 Chieti, Italy*

Antonella Fontana − *Department of Pharmacy, University of Chieti-Pescara "G. d'Annunzio", I-66010 Chieti, Italy;* orcid.org/0000-0002-5391-7520

Luca Madia − *EniProgetti S.p.A., 30175 Venice, Italy*

Massimo Zampato − *EniProgetti S.p.A., 30175 Venice, Italy*

Complete contact information is available at:
https://pubs.acs.org/10.1021/acssuschemeng.2c00994
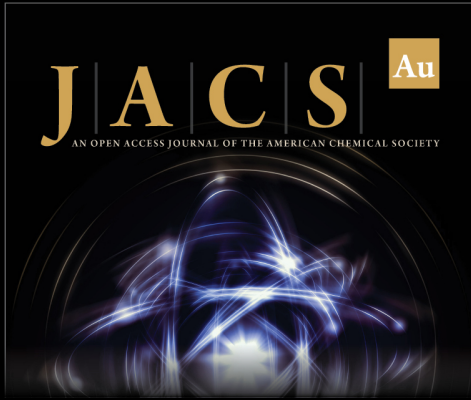
■ REFERENCES

(1) IRENA. World Energy Transitions Outlook. https://www.irena.org/publications/2021/Jun/World-Energy-Transitions-Outlook (June, 2021).

(2) Saeedi Dehaghani, A. H.; Badizad, M. H. Thermodynamic Modeling of Gas Hydrate Formation in Presence of Thermodynamic Inhibitors with a New Association Equation of State. *Fluid Phase Equilib.* **2016**, *427*, 328−339.

(3) Khan, M. S.; Lal, B.; Partoon, B.; Keong, L. K.; Bustam, A. B.; Mellon, N. B. Experimental Evaluation of a Novel Thermodynamic Inhibitor for CH4 and CO2 Hydrates. *Procedia Eng.* **2016**, *148*, 932−940.

(4) Zerpa, L. E.; Salager, J. L.; Koh, C. A.; Sloan, E. D.; Sum, A. K. Surface Chemistry and Gas Hydrates in Flow Assurance. *Ind. Eng. Chem. Res.* **2011**, *50*, 188−197.

(5) Tohidi, B.; Anderson, R.; Mozaffar, H.; Tohidi, F. The Return of Kinetic Hydrate Inhibitors. *Energy and Fuels* **2015**, *29*, 8254−8260.

(6) Kumar, A.; Sakpal, T.; Kumar, R. Influence of Low-Dosage Hydrate Inhibitors on Methane Clathrate Hydrate Formation and Dissociation Kinetics. *Energy Technol.* **2015**, *3*, 717−725.

(7) Perrin, A.; Musa, O. M.; Steed, J. W. The Chemistry of Low Dosage Clathrate Hydrate Inhibitors. *Chem. Soc. Rev.* **2013**, *42*, 1996−2015.

(8) Di Profio, P.; Canale, V.; Marvulli, F.; Zappacosta, R.; Fontana, A.; Siani, G.; Germani, R. Chemoinformatic Design of Amphiphilic Molecules for Methane Hydrate Inhibition. *J. Chemom.* **2018**, *32*, No. e3008.

(9) Kelland, M. A. *Production Chemicals for the Oil and Gas Industry*; CRC Press, 2014.

(10) Di Crescenzo, A.; Di Profio, P.; Siani, G.; Zappacosta, R.; Fontana, A. Optimizing the Interactions of Surfactants with Graphitic Surfaces and Clathrate Hydrates. *Langmuir* **2016**, *32*, 6559−6570.

(11) Sloan, E. D., Jr.; Koh, C. A. *Clathrate Hydrates of Natural Gases*; CRC Press, 2007.

(12) Dec, S. F.; Bowler, K. E.; Stadterman, L. L.; Koh, C. A.; Sloan, E. D. Direct Measure of the Hydration Number of Aqueous Methane. *J. Am. Chem. Soc.* **2006**, *128*, 414−415.

(13) Knott, B. C.; Molinero, V.; Doherty, M. F.; Peters, B. Homogeneous Nucleation of Methane Hydrates: Unrealistic under Realistic Conditions. *J. Am. Chem. Soc.* **2012**, *134*, 19544−19547.

(14) Jacobson, L. C.; Hujo, W.; Molinero, V. Amorphous Precursors in the Nucleation of Clathrate Hydrates. *J. Am. Chem. Soc.* **2010**, *132*, 11806−11811.

(15) Koga, T.; Wong, J.; Endoh, M. K.; Mahajan, D.; Gutt, C.; Satija, S. K. Hydrate Formation at the Methane/Water Interface on the Molecular Scale. *Langmuir* **2010**, *26*, 4627−4630.

(16) Hassanali, A.; Giberti, F.; Cuny, J.; Kühne, T. D.; Parrinello, M. Proton Transfer through the Water Gossamer. *Proc. Natl. Acad. Sci. U.S.A.* **2013**, *110*, 13723−13728.

(17) Mishra, P. K.; Vendrell, O.; Santra, R. Ultrafast Energy Transfer to Liquid Water by Sub-Picosecond High-Intensity Terahertz Pulses: An Ab Initio Molecular Dynamics Study. *Angew. Chem., Int. Ed.* **2013**, *52*, 13685−13687.

(18) Han, J. x.; Takahashi, L. K.; Lin, W.; Lee, E.; Keutsch, F. N.; Saykally, R. J. Terahertz Vibration-Rotation-Tunneling (VRT) Spectroscopy of the D6-Water Trimer: Complete Characterization of the 2.94 THz Torsional Band (Kn = ±21 ← 00). *Chem. Phys. Lett.* **2006**, *423*, 344−351.

(19) Lin, W.; Steyert, D. W.; Hlavacek, N. C.; Mukhopadhyay, A.; Page, R. H.; Siegel, P. H.; Saykally, R. J. Terahertz Vibration-Rotation-Tunneling Spectroscopy of the Propane-Water Dimer: The Ortho-State of a 20 Cm-1 Torsion. *Chem. Phys. Lett.* **2014**, *612*, 167−171.

(20) Atilhan, M.; Pala, N.; Aparicio, S. A Quantum Chemistry Study of Natural Gas Hydrates. *J. Mol. Model.* **2014**, *20*, 2182.

(21) Johnson, K. H. Methods and Systems for Extracting Gases. U.S. Patent USO169345A12002.

(22) Johnson, K.; Price-Gallagher, M.; Mamer, O.; Lesimple, A.; Fletcher, C.; Chen, Y.; Lu, X.; Yamaguchi, M.; Zhang, X. C. Water Vapor: An Extraordinary Terahertz Wave Source under Optical Excitation. *Phys. Lett. A* **2008**, *372*, 6037−6040.

(23) Zhu, X.-L.; Cao, J.-W.; Qin, X.-L.; Jiang, L.; Gu, Y.; Wang, H.-C.; Liu, Y.; Kolesnikov, A. I.; Zhang, P. Origin of Two Distinct Peaks of Ice in the THz Region and Its Application for Natural Gas Hydrate Dissociation. *J. Phys. Chem. C* **2020**, *124*, 1165−1170.

(24) Wang, H.-C.; Zhu, X.-L.; Cao, J.-W.; Qin, X.-L.; Yang, Y.-C.; Niu, T.-X.; Lu, Y.-B.; Zhang, P. Density Functional Theory Studies of Hydrogen Bonding Vibrations in SI Gas Hydrates. *New J. Phys.* **2020**, *22*, No. 093066.

(25) Kristensen, T. T.; Withayachumnankul, W.; Jepsen, P. U.; Abbott, D. Modeling Terahertz Heating Effects on Water. *Opt. Express* **2010**, *18*, 4727−4739.

(26) Lunkenheimer, P.; Emmert, S.; Gulich, R.; Köhler, M.; Wolf, M.; Schwab, M.; Loidl, A. Electromagnetic-Radiation Absorption by Water. *Phys. Rev. E* **2017**, *96*, No. 062607.

(27) Hölzl, C.; Forbert, H.; Marx, D. Dielectric Relaxation of Water: Assessing the Impact of Localized Modes, Translational Diffusion, and Collective Dynamics. *Phys. Chem. Chem. Phys.* **2021**, *23*, 20875−20882.

(28) Teravil. Terahertz Emitter. http://www.teravil.lt/emitter.php (June, 2021).

(29) CSMHYD. http://hydrates.mines.edu/CHR/Software.html (June, 2021).

(30) Kelland, M. A.; Magnusson, C.; Lin, H.; Abrahamsen, E.; Mady, M. F. Acylamide and Amine Oxide Derivatives of Linear and Hyperbranched Polyethylenimine. Part 2: Comparison of Gas Kinetic Hydrate Inhibition Performance. *Energy Fuels* **2016**, *30*, 5665−5671.

(31) Canale, V.; Fontana, A.; Siani, G.; Di Profio, P. Hydrate Induction Time with Temperature Steps: A Novel Method for the Determination of Kinetic Parameters. *Energy and Fuels* **2019**, *33*, 6113−6118.

(32) Yu, B. L.; Yang, Y.; Zeng, F.; Xin, X.; Alfano, R. R. Reorientation of the H2 O Cage Studied by Terahertz Time-Domain Spectroscopy. *Appl. Phys. Lett.* **2005**, *86*, No. 061912.

(33) Tsubouchi, M.; Hoshina, H.; Nagai, M.; Isoyama, G. Plane Photoacoustic Wave Generation in Liquid Water Using Irradiation of Terahertz Pulses. *Sci. Rep.* **2020**, *10*, No. 18537.

(34) Apostol, M. Coherence Domains in Matter Interacting with Radiation. *Phys. Lett. A* **2009**, *373*, 379−384.

(35) Apostol, M.; Ganciu, M. Coherent Polarization Driven by External Electromagnetic Fields. *Phys. Lett. A* **2010**, *374*, 4848−4852.

(36) Elton, D. C.; Fernández-Serra, M. The Hydrogen-Bond Network of Water Supports Propagating Optical Phonon-like Modes. *Nat. Commun.* **2016**, *7*, No. 10193.

(37) Ball, P.; Hallsworth, J. E. Water Structure and Chaotropicity: Their Uses, Abuses and Biological Implications. *Phys. Chem. Chem. Phys.* **2015**, *17*, 8297−8305.